


Constant of motion for ideal grain growth in three dimensionsE. Eren and J. K. Mason ^{*}*Department of Materials Science and Engineering, University of California, Davis, California 95616, USA*

(Received 23 August 2021; accepted 13 October 2021; published 22 October 2021)

Most metallic and ceramic materials are comprised of space-filling collections of crystalline grains separated by grain boundaries. While this grain structure has been studied for more than a century, there are few rigorous results regarding its global properties available in the literature. We present a rigorous result for three-dimensional grain structures that relates the integral of the Gaussian curvature over the grain boundaries to the numbers of grains and quadruple junctions. The result is numerically verified for a grain structure consisting of periodic truncated octahedra.

DOI: [10.1103/PhysRevB.104.L140103](https://doi.org/10.1103/PhysRevB.104.L140103)

The grain structure of polycrystalline materials is deceptively simple, and for that reason has been the subject of intense and ongoing study. For specificity, consider a model system where the grain boundary energy and mobility are constants, i.e., do not depend on grain misorientation or the boundary plane normal. The phenomenological Turnbull equation [1] relates the normal velocity of a grain boundary in such a system to the driving pressure, and along with the Young-Laplace equation [2], suggests that the normal velocity is directly proportional to the mean curvature of the grain boundary. The migration of individual boundaries induces the evolution of the grain structure, a process known as grain growth, where the total area of grain boundaries and the number of grains decrease with time.

There are surprisingly few rigorous results known about grain structures, even for the two-dimensional version of this system. Energy considerations require that grain boundaries only meet at triple junctions with internal angles of $2\pi/3$ [3,4]. A consequence of this and curvature-driven grain growth is that a grain's area changes at a rate that depends only on the number of bounding vertices [5,6]. Globally, topological arguments require that the average number of such bounding vertices be precisely six [7]. There are natural analogs to several, but not all, of these results in three dimensions. Grain boundaries only meet at triple junction lines with dihedral angles of $2\pi/3$, and triple junction lines only meet at quadruple junction points with angles of $\cos^{-1}(-1/3)$ [3,4]. The rate of volume change of a grain depends not only on the total length of the bounding triple lines, but on a measure of the linear dimension known as the mean width [8,9]. For both the two- and three-dimensional systems, the hypothesis that the structure reaches a statistically self-similar state implies that the average grain diameter increases as the square root of time [10,11]. This is the effective extent of current knowledge.

There have been a variety of inexact relationships proposed as well, usually for grain structures in the conjectured self-

similar state [12]. Ones that relate to the global properties of the three-dimensional system include proposed distributions for the effective radius of a grain [13–15] and the number of faces bounding a grain [15]. Recent advances in several microscopy techniques promise to make three-dimensional grain structure data more readily available, possibly allowing such relationships to be further refined. Three-dimensional electron backscatter diffraction [16,17] destructively images the grain structure by a serial sectioning process, whereas three-dimensional x-ray diffraction microscopy [18,19] is nondestructive but generally offers poorer spatial resolution. Given this situation, additional rigorous results for the global properties of the grain structure of the model three-dimensional system would be valuable, both to measure deviations of the experimental systems from the model one, and to verify the accuracy of grain structures generated by computational means. This Letter proves one such result, relating the integral of the Gaussian curvature over the grain boundaries to the numbers of grains and quadruple junction points, and thereby to the numbers of grain boundaries and triple junction lines.

Let Ω be a space-filling grain structure composed of grains that meet in twos on grain boundaries, grain boundaries that meet in threes at triple junction lines, and triple junction lines that meet in fours at quadruple junction points, as in Fig. 1. Further suppose that Ω satisfies Plateau's laws [i.e., grain boundaries meet at dihedral angles of $2\pi/3$ and triple junction lines meet at angles of $\cos^{-1}(-1/3)$], and that Ω is defined in a three-dimensional region with periodic boundary conditions. If G is a grain in Ω , then our main result is that the expectation value of the Gaussian curvature K integrated over the interiors of the grain boundaries of G and the expectation value of the number of quadruple junction points $f_0(G)$ of G are related by

$$\left\langle \int_{\partial G} K dA \right\rangle = 4\pi - \alpha \langle f_0(G) \rangle. \quad (1)$$

The angle brackets indicate an average performed over all grains in Ω , ∂G indicates the interiors of the grain boundaries of G , and $\alpha = 2\pi - 3 \cos^{-1}(-1/3)$ is the angular defect at a quadruple junction point. This result is exact (given a

*jkmason@ucdavis.edu

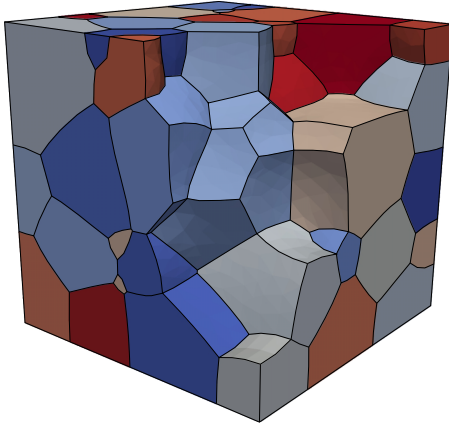


FIG. 1. A grain structure in a cubic volume, with several grains removed to reveal the interior. Color indicates the individual grains, internal curved surfaces are grain boundaries, internal black lines are triple junction lines, and four triple junction lines intersect at quadruple junction points

few technical assumptions that are usually satisfied and are discussed in the Supplemental Material [20]), and to our knowledge does not appear in the literature; a related result by Kusner [21] requires that all the grain boundaries be minimal surfaces, and one by Glicksman [22] applies only to unconstructable grain structures of average n -polyhedra.

The Gaussian curvature of a surface is defined as the product of the principal curvatures at any point. The appearance of this quantity in Eq. (1) could be surprising, since the mean curvature (the sum of the principal curvatures) is the one that controls the dynamics of the grain boundary network [1,2]. That said, the Gaussian curvature is in some ways the more fundamental of the two quantities, being an intrinsic property of the surface that does not depend on the way the surface is embedded in Euclidean space. For example, the Gaussian curvature of a sheet of paper is zero at every point whether the sheet is laid flat or rolled up, though the same is not true for the mean curvature. This invariance to the embedding is reflected in the celebrated Gauss-Bonnet theorem:

$$\int_{\partial G} K dA + \sum_{i=1}^{f_2(G)} \int_{\partial F_i} \kappa_g ds + \sum_{i=1}^{f_0(G)} \alpha_i = 2\pi \chi(\partial G).$$

While this version specifically applies to the surface of a grain, all versions relate the integrated Gaussian curvature of a surface to its Euler characteristic $\chi(\partial G)$ (equal to two when the surface can be smoothly deformed into a sphere without cutting or gluing). The terms on the left include the integrated Gaussian curvature over the grain boundary interiors, the sum of the integrated geodesic curvature κ_g over the interiors of the bounding triple junction lines ∂F_i of all grain boundaries F_i , and the sum of the angular defects α_i of the quadruple junction points of G .

If G can be smoothly deformed into a sphere and belongs to a grain structure Ω that obeys Plateau's rules, then this can be simplified to

$$\int_{\partial G} K dA + \sum_{i=1}^{f_1(G)} \int_{E_i} \kappa \mathbf{e}_2 \cdot \mathbf{v} ds + \alpha f_0(G) = 4\pi,$$

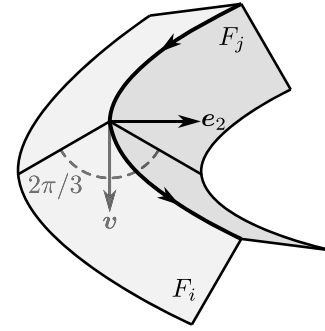


FIG. 2. Grain boundaries F_i and F_j meet at the triple junction line in bold, and \mathbf{v} bisects the dihedral angle between F_i and F_j . Arrows indicate the tangent direction, and the second Frenet vector \mathbf{e}_2 points along the triple junction line's normal direction.

where the most significant change is to the middle term on the left; this is now the sum of the integrated curvature of the triple junction lines of G , weighted by the dot product of the second Frenet vector \mathbf{e}_2 of the curve and a unit vector \mathbf{v} that bisects the dihedral angle between the adjoining grain boundaries; see Fig. 2. Summing this equation over all grains in Ω results in a remarkable cancellation (previously noted by DeHoff [23]) where the contribution of the second term on the left vanishes. Specifically, every triple junction line is integrated over three times, once for each adjoining grain. $\kappa \mathbf{e}_2$ is an inherent quantity of the triple junction line that is the same for all three integrals, but the three \mathbf{v} are all unit vectors in a plane with mutual angles of $2\pi/3$. That is, the sum of the three \mathbf{v} vanishes identically for each triple junction line, leaving an alternative version of the main result,

$$\sum_{i=1}^{f_2(\Omega)} \int_{F_i} K dA = 2\pi f_3(\Omega) - 2\alpha f_0(\Omega), \quad (2)$$

where F_i is the i th grain boundary of Ω and $f_0(\Omega)$, $f_2(\Omega)$, and $f_3(\Omega)$ are the numbers of quadruple junction points, grain boundaries, and grains of Ω . Dividing through by $f_3(\Omega)$ and multiplying by a constant gives Eq. (1). More detailed derivations of both Eqs. (1) and (2) are provided in the Supplemental Material [20].

Although Eq. (1) appears to be simpler, there are at least two observations that are more clearly made by means of Eq. (2). The first is that the integral of K over the grain boundaries of Ω depends only on the numbers of grains and quadruple junction points of Ω , and not on the geometry of the grain structure. That is, the left-hand side of Eq. (2) is invariant to any deformation of Ω that preserves the numbers of grains and quadruple junction points. The second is that a sufficiently accurate measurement of the integral of K over the grain boundaries of Ω in principle specifies the numbers of all components of Ω . Observe that since there is no rational number that relates the coefficients of $f_3(\Omega)$ and $f_0(\Omega)$ in Eq. (2), the numbers of grains and quadruple junctions can be inferred if the left-hand side is known sufficiently accurately. The number of triple junction lines can then be found from $2f_1(\Omega) = 4f_0(\Omega)$ by a counting argument, and the number of grains from $0 = f_0(\Omega) - f_1(\Omega) + f_2(\Omega) - f_3(\Omega)$ which follows from the domain of Ω being a three-torus with

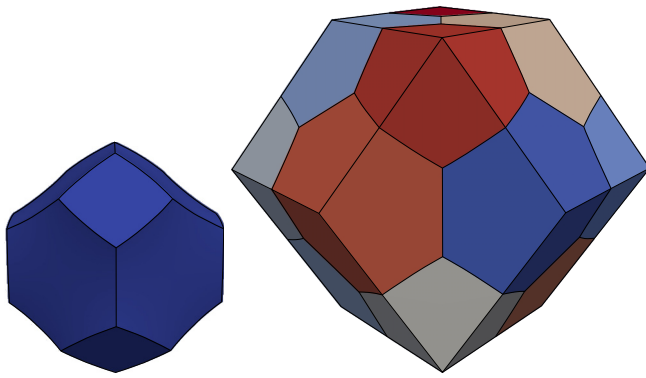


FIG. 3. An infinite periodic grain structure that satisfies Plateau’s laws can be constructed by repeating a relaxed truncated octahedron (left). This grain was found by starting with a periodic unit of a grain structure consisting of unrelaxed truncated octahedra, fixing the location of the interior quadruple junction points, and minimizing the grain boundary area (right).

$\chi(\Omega) = 0$. The necessary modifications to Eqs. (1) and (2) for grain structures in other domains (e.g., ones with free boundaries) are discussed in the Supplemental Material [20].

As a numerical confirmation of Eq. (1), consider a grain structure consisting of periodic truncated octahedra, relaxed under the action of surface tension to satisfy Plateau’s laws; one such grain is shown on the left of Fig. 3. The shape of this grain was found by starting with a grain structure consisting of unrelaxed truncated octahedra and constructing the periodic unit shown on the right of Fig. 3, with a single grain at the center and corners at the centers of the neighboring grains. The periodic unit was computationally represented by a volumetric finite element mesh with linear elements, with the average number of triangles per hexagonal face n_t depending on a characteristic length and the details of the mesh adaptation algorithm. The locations of the interior quadruple junction points were fixed, and the structure was relaxed by allowing the vertices on grain surfaces to move according to equations of motion known to reproduce curvature-driven grain growth [24] until the magnitude of the vertex forces fell below a threshold. The grain structure did not reach a steady-state configuration when the locations of the interior quadruple junction points were not fixed, owing to a known instability of this grain structure to volumetric perturbations [25]. While quadratic elements would allow the steady-state geometry to be more accurately represented, a convergence analysis with an increasing number of linear elements is sufficient for the present purpose.

The simulations were performed with a modified version of a recently developed microstructure evolution code [26] that usually uses SCOREC [27] for mesh management and maintenance, but the mesh adaptation operations were found to interfere with the convergence of the grain geometry. Instead, artificial vertex forces defined by Kuprat [28] were used to maintain the mesh element quality during the structure relaxation. Since the artificial forces only acted on vertices on the grain interiors, it is expected that they did not substantially affect the grain geometry. The boundary conditions were defined to make the simulation cell behave as a periodic unit in

a grain structure consisting of periodic truncated octahedra. Whereas the grain boundaries on the simulation cell interior had a constant nonzero energy per unit area, the external surfaces of the simulation cell were assigned zero energy per unit area; this is consistent with viewing them as the result of intersecting grains in the underlying grain structure with the boundary of the periodic unit. Vertices on the external surfaces were constrained to remain on the external surfaces during relaxation by projecting away any displacement in the normal direction, effectively imposing a Neumann boundary condition. The integrated Gaussian curvature was calculated as the sum of the angular defects at the vertices on the grain boundary interiors, where the angular defect is defined as 2π minus the sum of the interior angles of the grain boundary triangles meeting at the vertex.

Table I shows the results of this analysis for increasing refinement of the mesh, i.e., as a function of n_t . The geometric accuracy of the representation can be evaluated by means of the percent reduction in grain boundary area ΔA of the relaxed truncated octahedron relative to the unrelaxed one. A detailed analysis [29] suggests a value of 0.159% for the continuous system; that ΔA does not converge to this value is likely due to the irregularity of the mesh. As for the integrated Gaussian curvature, the average quantities in Eq. (1) are equivalent to those for a single grain by periodicity. This implies that the integral of the Gaussian curvature over the interiors of the grain boundaries should be

$$\int_{\partial G} K dA = 4\pi - 24\alpha \approx -0.664484.$$

A conjugate gradient minimization algorithm and bootstrapping were used to fit the model $\int K dA = a + bn_t^c$ to the data in Table I, giving $a = -0.661 \pm 0.022$, $b = 2.08 \pm 0.51$, and $c = -0.378 \pm 0.060$ (reported as the medians and half the interquartile range). This implies that the integrated Gaussian curvature would be -0.661 ± 0.022 in the $n_t \rightarrow \infty$ limit, and is interpreted as numerically confirming Eq. (1) given the degree of approximation of the grain geometry. That the integrated Gaussian curvature converges to the expected value even though the percent area reduction does not confirm the assertion that Eqs. (1) and (2) are invariant to geometric perturbations of the structure, provided the numbers of grains and quadruple junction points remain the same and Plateau’s laws are satisfied.

Alternatively, one could consider the feasibility of inferring $f_3(\Omega)$ and $f_0(\Omega)$ by means of a sufficiently accurate measurement of the integral of K over the grain boundaries of Ω in Eq. (2). This can be done by a graphical construction in the plane with $f_3(\Omega)$ and $f_0(\Omega)$ on the vertical and horizontal axes. Given the integral of the Gaussian curvature over the grain boundaries of Ω , Eq. (2) defines a line in this plane with an irrational slope. Since the actual values of $f_3(\Omega)$ and $f_0(\Omega)$ are necessarily positive integers, this line passes through exactly one point on the integer lattice in the positive quadrant. In practice, any error in the measurement of the integrated Gaussian curvature would change the intercept with the vertical axis and shift the line off of the lattice point; whether this is an issue or not depends on the magnitude of the error and any *a priori* bounds that can be placed on

TABLE I. The percent grain boundary area change of the relaxed truncated octahedron relative to the unrelaxed one and the integrated Gaussian curvature of the relaxed truncated octahedron as functions of n_t .

n_t	61	129	477	665	1885	2610	3250	4314	5322	6532	7649	8906
ΔA (%)	0.0863	0.129	0.135	0.136	0.136	0.137	0.136	0.136	0.136	0.136	0.136	0.136
$\int K dA$	-0.219	-0.349	-0.461	-0.477	-0.544	-0.554	-0.563	-0.568	-0.578	-0.588	-0.593	-0.597

$f_3(\Omega)$ and $f_0(\Omega)$. For example, Fig. 4 shows this construction for the data in Table I with the constraints $3 \leq f_3(\Omega) \leq 5$ and $20 \leq f_0(\Omega) \leq 28$. Since the magnitude of the error is assumed to be unknown, it is reasonable to suppose that the correct values of $f_3(\Omega)$ and $f_0(\Omega)$ correspond to the integer lattice point closest to the line within the feasible region. This procedure correctly identifies the relevant integer lattice point as (24, 4) for $n_t \geq 477$; in general, the effect of integrated Gaussian curvature error is reduced as the area of the feasible region decreases.

Apart from advancing our fundamental understanding of grain structures, there remains the question of the practical utility of Eqs. (1) and (2) (and the analogs in the Supplemental Material [20]). This question is made more pressing by there being few materials that actually evolve by the relevant ideal grain growth process; the grain boundary energy and mobility do generally depend on the grain misorientation and boundary plane normal, but in a way that is not precisely known even for simple model systems. The only way to conceivably measure grain boundary mobility is by a time series of three-dimensional microstructures, visualized using a non-destructive technique. While such techniques exist [18,19], fitting to such data has not yet yielded single-valued mobilities [30], perhaps due to insufficient experimental resolution or confounding variables. As for grain boundary energies, despite the seminal work of Morawiec [31] indicating how the grain boundary energies could in principle be extracted from a three-dimensional microstructure, the grain boundary energies for, e.g., simple metals are not yet widely available in the literature. Finally, simulations of grain boundary properties [32–35] out of necessity only consider a small subset of possible grain boundary characters, and cannot be validated in the absence of reliable experimental data.

Given this situation, the authors propose two possible applications of this Letter's results based on the differences of

the left and right sides of Eqs. (1) and (2):

$$e_1 = \left\langle \int_{\partial G} K dA \right\rangle - 4\pi + \alpha \langle f_0(G) \rangle,$$

$$e_2 = \sum_{i=1}^{f_2(\Omega)} \int_{F_i} K dA - 2\pi f_3(\Omega) + 2\alpha f_0(\Omega).$$

First, e_1 and e_2 could be used as rough measures of the deviation of a physical system from an ideal one (along with other quantities such as the grain growth exponent and the grain size distribution), thereby contributing to the ongoing investigation of how severe is the assumption of ideal grain growth in practice. Second, there is widespread interest in generating microstructures (for use in, e.g., integrated computational materials engineering) by means of physics-based simulations of microstructure evolution. Faced with the absence of reliable grain boundary data, such simulations generally assume that grain boundary properties are constants, making this Letter's results relevant to the vast majority of contemporary microstructure evolution codes. In this context, e_1 and e_2 could be used to evaluate the accuracy of the geometric representation of a grain structure; the derivation above suggests that these quantities should be particularly sensitive to the geometry around triple junction lines and quadruple junction points. Since the angle conditions around triple junction lines are directly implicated in the rates of area and volume change of two-dimensional [5,6] and three-dimensional [8,9] grains, any deviations from Eqs. (1) and (2) could function as bounds on the maximum achievable accuracy of simulations of mean-curvature driven grain growth.

The authors are grateful to R. D. MacPherson for enlightening discussions about grain structure geometry. E.E. and J.K.M. were supported by the National Science Foundation under Grant No. 1839370.

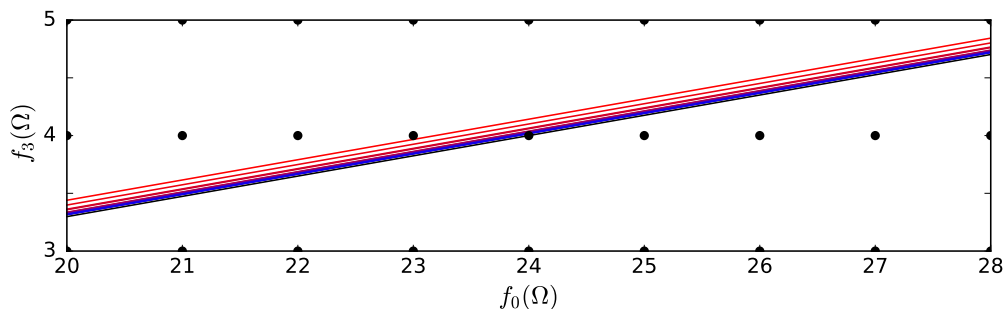


FIG. 4. The lines defined by Eq. (2) for the data in Table I in the feasible region $3 \leq f_3(\Omega) \leq 5$ and $20 \leq f_0(\Omega) \leq 28$. The lines are colored from red to blue with decreasing error and the black line passing through (24, 4) corresponds to the exact solution. The closest integer lattice point to the line is (24, 4) for $n_t \geq 477$.

J.K.M. conceived the study, developed the mathematics, and analyzed the numerical results. E.E. designed and im-

plemented the simulation model and performed the numerical experiments. J.K.M. and E.E. jointly prepared the manuscript.

-
- [1] D. Turnbull, Theory of grain boundary migration rates, *J. Met.* **3**, 661 (1951).
- [2] P. S. Laplace, *Supplément au dixième livre du traité de mécanique céleste sur l'action capillaire* (De L'Imprimerie de Crapelet, Paris, 1805), Vol. 6.
- [3] J. A. F. Plateau, *Statique expérimentale et théorique des liquides soumis aux seules forces moléculaires* (Gauthier-Villars, Paris, 1873), Vol. 2.
- [4] J. E. Taylor, The structure of singularities in soap-bubble-like and soap-film-like minimal surfaces, *Ann. Math.* **103**, 489 (1976).
- [5] J. von Neumann, in *Metal Interfaces* (American Society for Metals, Cleveland, 1952), p. 108.
- [6] W. W. Mullins, Two-dimensional motion of idealized grain boundaries, *J. Appl. Phys.* **27**, 900 (1956).
- [7] C. S. Smith, Some elementary principles of polycrystalline microstructure, *Metall. Rev.* **9**, 1 (1964).
- [8] J. W. Cahn, Significance of average mean curvature and its determination by quantitative metallography, *Trans. Metall. Soc. AIME* **239**, 610 (1967).
- [9] R. D. MacPherson and D. J. Srolovitz, The von Neumann relation generalized to coarsening of three-dimensional microstructures, *Nature (London)* **446**, 1053 (2007).
- [10] W. Mullins, The statistical self-similarity hypothesis in grain growth and particle coarsening, *J. Appl. Phys.* **59**, 1341 (1986).
- [11] H. Atkinson, Overview No. 65: Theories of normal grain growth in pure single phase systems, *Acta Metall.* **36**, 469 (1988).
- [12] J. K. Mason, E. A. Lazar, R. D. MacPherson, and D. J. Srolovitz, Geometric and topological properties of the canonical grain-growth microstructure, *Phys. Rev. E* **92**, 063308 (2015).
- [13] M. Hillert, On the theory of normal and abnormal grain growth, *Acta Metall.* **13**, 227 (1965).
- [14] W. Fayad, C. Thompson, and H. Frost, Steady-state grain-size distributions resulting from grain growth in two dimensions, *Scr. Mater.* **40**, 1199 (1999).
- [15] P. Rios and M. Glicksman, Polyhedral model for self-similar grain growth, *Acta Mater.* **56**, 1165 (2008).
- [16] M. D. Uchic, M. Groeber, R. Wheeler IV, F. Scheltens, and D. M. Dimiduk, Augmenting the 3D characterization capability of the dual beam FIB-SEM, *Microsc. Microanal.* **10**, 1136 (2004).
- [17] J. Konrad, S. Zaeferrer, and D. Raabe, Investigation of orientation gradients around a hard laves particle in a warm-rolled Fe₃Al-based alloy using a 3D EBSD-FIB technique, *Acta Mater.* **54**, 1369 (2006).
- [18] H. F. Poulsen, *Three-Dimensional X-ray Diffraction Microscopy: Mapping Polycrystals and their Dynamics* (Springer, Berlin, 2004), Vol. 205.
- [19] S. Li and R. Suter, Adaptive reconstruction method for three-dimensional orientation imaging, *J. Appl. Cryst.* **46**, 512 (2013).
- [20] See Supplemental Material at <http://link.aps.org/supplemental/10.1103/PhysRevB.104.L140103> which includes Ref. [36] for a more detailed derivation of Eqs. (1) and (2), and a discussion on general boundary conditions.
- [21] R. Kusner, The number of faces in a minimal foam, *Proc. R. Soc. London, Ser. A* **439**, 683 (1992).
- [22] M. Glicksman, Analysis of 3-D network structures, *Philos. Mag.* **85**, 3 (2005).
- [23] R. DeHoff, The spherical image concept applied to grain structures, *Acta Metall. Mater.* **42**, 2633 (1994).
- [24] J. K. Mason, Stability and motion of arbitrary grain boundary junctions, *Acta Mater.* **125**, 286 (2017).
- [25] D. Levine, Stability of monodisperse dry foams, *Philos. Mag. Lett.* **74**, 303 (1996).
- [26] E. Eren and J. K. Mason, Topological transitions during grain growth on a finite element mesh, *Phys. Rev. Materials* **5**, 103802 (2021).
- [27] D. A. Ibanez, E. S. Seol, C. W. Smith, and M. S. Shephard, PUMI: Parallel unstructured mesh infrastructure, *ACM Trans. Math. Software* **42**, 17 (2016).
- [28] A. Kuprat, Modeling microstructure evolution using gradient-weighted moving finite elements, *SIAM J. Sci. Comput.* **22**, 535 (2000).
- [29] D. A. Reinelt and A. M. Kraynik, Large elastic deformations of three-dimensional foams and highly concentrated emulsions, *J. Colloid Interface Sci.* **159**, 460 (1993).
- [30] J. Zhang, W. Ludwig, Y. Zhang, H. H. B. Sørensen, D. J. Rowenhorst, A. Yamanaka, P. W. Voorhees, and H. F. Poulsen, Grain boundary mobilities in polycrystals, *Acta Mater.* **191**, 211 (2020).
- [31] A. Morawiec, Method to calculate the grain boundary energy distribution over the space of macroscopic boundary parameters from the geometry of triple junctions, *Acta Mater.* **48**, 3525 (2000).
- [32] F. Ulomek and V. Mohles, Molecular dynamics simulations of grain boundary mobility in Al, Cu and γ -Fe using a symmetrical driving force, *Modell. Simul. Mater. Sci. Eng.* **22**, 055011 (2014).
- [33] F. Ulomek, C. O'Brien, S. Foiles, and V. Mohles, Energy conserving orientational force for determining grain boundary mobility, *Modell. Simul. Mater. Sci. Eng.* **23**, 025007 (2015).
- [34] D. L. Olmsted, S. M. Foiles, and E. A. Holm, Survey of computed grain boundary properties in face-centered cubic metals: I. Grain boundary energy, *Acta Mater.* **57**, 3694 (2009).
- [35] S. Ratanaphan, D. L. Olmsted, V. V. Bulatov, E. A. Holm, A. D. Rollett, and G. S. Rohrer, Grain boundary energies in body-centered cubic metals, *Acta Mater.* **88**, 346 (2015).
- [36] A. Gray, E. Abbena, and S. Salamon, *Modern Differential Geometry of Curves and Surfaces with Mathematica®* (Chapman and Hall/CRC, New York, 2017).